Regulation theory: review and digital regulation

F. Bordry
CERN, Geneva, Switzerland

Abstract

This paper reviews system modelling and regulation loops design. Continuous and discrete time domains are presented. The concept of discrete time model is introduced and the choice of the sampling frequency is highlighted. This approach takes advantage of the digital controller's capacity to treat complex algorithms. A general method to decouple multi-input, multi-output systems is described and illustrated with the LHC inner triplet powering system.

1   Introduction

The purpose of a power converter is to process and control the flow of electric energy by supplying voltages and currents in a form that is optimally suited for user loads. Therefore, regulation design and implementation are part of the design and construction of any power converter.

The fast development of digital electronics has changed the approach. Its performance and flexibility make it suitable for power converter regulation. However, it is not enough to reproduce the analog controller PID characteristics.

This paper does not aim to describe control theory in a systematic and exhaustive way; numerous books and handbooks exist in this domain.

In the first part, continuous-time control techniques are quickly recalled. For power converters, it is important to study the rejection of perturbations arising mainly from the electrical network.

Digital control is presented in the second part. The concept of discrete-time model is introduced and the choice of the sampling frequency, which is defined in accordance with the desired closed-loop bandwidth, does not match the analog approach.

Before presenting the regulation loops used for the LHC power converters, the terms used to define the precision of a power converter are given.

Finally, the method used to transform a Multiple Input Multiple Output (MIMO) into a Single Input Single Output (SISO) is illustrated with the example of the LHC inner triplet powering system.

2   Basic review

The domain of linear and non-linear control theory is a wide domain and an important part of electrical engineering training. Numerous books, handbooks and papers cover this field (see Refs. [1] to [2]). The aim of this paper is to review briefly the main concepts of system models and their characteristics.

2.1   Continuous-time models

Since 1970, the use of 'classical' or frequency domain methods (Bode, Nyquist, Evans), which have played such an important role with respect to single input-output (scalar) systems, has evolved to the

more 'modern' state-space approach. This evolution could be attributed to the increasing complexity of systems requiring control and the need (or desire) to 'optimize' their performance.

The behaviour of a system to be regulated is described by a dynamic model expressed in the more general case of a multi-input, multi-output system by the following state equations:

$$\frac{\mathrm{d}X}{\mathrm{d}t} = F\left[X(t), U(t)\right] \text{ with } X(t_0) = X(0) \tag{1}$$

$$Y(t) = G\left[X(t),\ U(t)\right], \tag{2}$$

in which $U(t)$ is the input vector (p inputs), $Y(t)$ is the output vector (m outputs) and $X(t)$ is the state vector (n states). The set of these two equations of the form (1-2) is called a dynamic equation. Equation (1) is the state equation and Eq. (2) is the output equation

In the case of a linear system, the dynamic equations become:

$$\frac{\mathrm{d}X}{\mathrm{d}t} = A(t) \cdot X(t) + B(t) \cdot U(t) \tag{3}$$

$$Y(t) = C(t) \cdot X(t) + D(t) \cdot U(t). \tag{4}$$

The matrices *A*, *B*, *C* and *D* are the state matrices.

If the characteristics of a system do not change with time, then the system is said to be time-invariant, fixed or stationary. In this case, the state matrices are independent of *t* and the dynamic equations are called linear time-invariant dynamic equations or fixed equations.

In the study of linear time-invariant systems, it is possible to apply the Laplace transform. Taking the Laplace transform of the fixed equations and assuming $X(0) = X_0$, we obtain:

$$s X(s) - X_0 = A \cdot X(s) + B \cdot U(s) \tag{5}$$

$$Y(s) = C \cdot X(s) + D \cdot U(s), \tag{6}$$

where the Laplace transform of a vector is, for example, for the state vector:

$$X(s) = \int_0^\infty X(t) \cdot e^{-st} dt. \tag{7}$$

From Eqs. (5) and (6), we have

$$X(s) = (sI - A)^{-1} \cdot X_0 + (sI - A)^{-1} \cdot B \cdot U(s) \tag{8}$$

$$Y(s) = C(sI - A)^{-1} \cdot X_0 + C(sI - A)^{-1} \cdot B \cdot U(s) + D \cdot U(s). \tag{9}$$

Equations (8) and (9) are algebraic equations. If X_0 and $U(s)$ are known, $X(s)$ and $Y(s)$ can be computed from Eqs. (8) and (9). If the initial state X_0 is null, the system is relaxed at $t = 0$; then the equation reduces to:

$$Y(s) = \left[C(sI - A)^{-1} \cdot B + D \right] \cdot U(s) = H(s) \cdot U(s), \tag{10}$$

where $H(s) = C(sI - A)^{-1} \cdot B + D$ is called the transfer-function matrix.

In the case of mono-input mono-output, differential equations are also often used to describe a system. Equations (11) and (12) illustrate this case for the 1st and 2nd order systems:

$$\frac{dy}{dt} = -\frac{y(t)}{T} + \frac{G}{T} u(t) \tag{11}$$

$$\frac{d^2 y(t)}{dt^2} + \frac{2 \cdot z \cdot w_0 \cdot dy(t)}{dt} + w_0^2 \cdot y(t) = w_0^2 \cdot u(t). \tag{12}$$

2.2 Controllability and observability

It is important to note that the three representations (state variable, differential equations, and transfer functions) are not equivalent in the case where all the states of the system are not observable or controllable. The state equation is the most general representation, as it takes into account all the modes regardless of their controllability or observability. The transfer function representation does not retain any non-controllable or non-observable modes.

A definition of the controllability of a system is that the system is controllable at any time t_0 if for any state $X(t_0)$ in the state space and any state X in the state space, it exists a finite time $t_1 > t_0$ and an input $U[t_0, t_1]$ that will transfer the state $X(t_0)$ to the state X at time t_1.

It is important to understand the previous formal definition. If it is theoretically possible to define an input signal which transfers in a finite time a state vector of a system from one value to any other value, nothing is stated about the energy which should be provided or about the system limitations (saturations, mechanical or electrical constraints, etc.). We shall come back to this point in Section 3.1.

The concept of observability is dual to that of controllability. Controllability deals with the possibility of steering the state from the input; observability with the possibility of estimating the state from the output. If a dynamic equation is controllable, all the modes of the equation can be excited from the input; if a dynamic equation is observable, all the modes of the equation can be observed from the output. These two concepts are defined under the assumption that we know completely the parameters of the system model (that is all the state matrices A, B, C and D are known).

The system is observable at any time t_0, if for any state $X(t_0)$ in the state space, a finite time $[t_0, t_1]$ exists such that the knowledge of the input $U[t_0, t_1]$ and of the output $Y[t_0, t_1]$ over the time interval $[t_0, t_1]$ suffices to determine the state $X(t_0)$. The observability of a system allows replacing physical transducers (costly or difficult to implement) by dynamic equations called observer [3].

Figure 1 shows a system with non-controllable states (X3 and X4) and non-observable states (X2 and X4). If these system modes are unstable (example of X3 and X4) or their dynamic is not acceptable, the system structure must be modified by the addition of transducers (non-observable modes) and actuators (non-controllable modes).
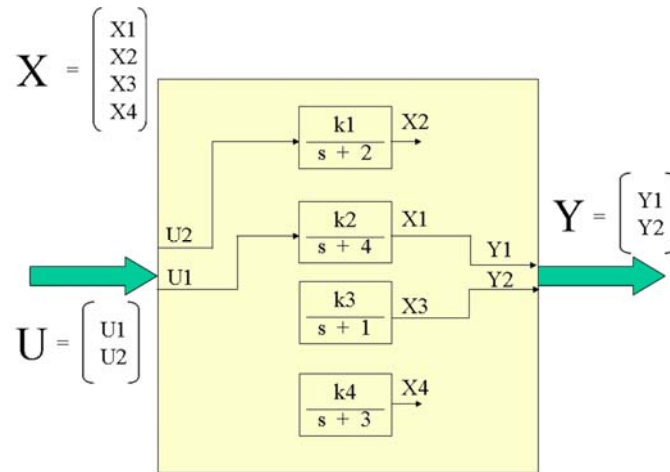
Fig.1: Example of a system with non-controllable and non-observable states

2.3   Stability

The evolution of the state vector X is obtained by the following equation.

$$X(t) = e^{A(t-t_0)} \cdot X(t_0) + \int_{t_0}^{t} e^{A(t-\tau)} \cdot B \cdot U(\tau) d\tau. \tag{13}$$

Both terms correspond, respectively, to the free-state response (independent of the input vector) and the forced-state response. The eigenvalues of the state matrix A determine the dynamics of the system.

From Eq. (13), the stability of the system can be deduced:

$$\lim_{t \to \infty} e^{A(t-t_0)} \cdot X(t_0) = 0. \tag{14}$$

The system is stable if the sign of the real part of A eigenvalues is negative.

2.4   Time responses

The response of a dynamic system to a step input is studied and characterized. Figure 2 shows the response of a stable system. This figure shows the parameters usually used to characterize the step response.
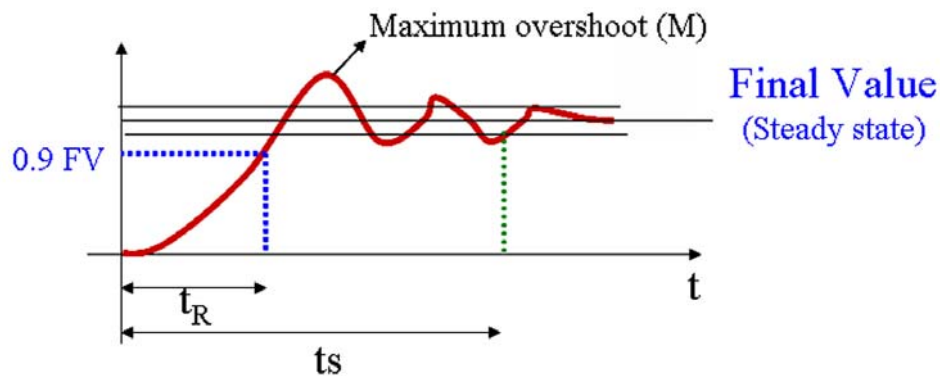

Fig. 2: Step response of a dynamic system

These parameters are

- t_R: **rise time**; defined as the time needed to attain 90% of the final value; or as the time needed for the output to increase from 10% to 90% of the final value

- t_S: **settling time**; defined as the time needed for the output to reach and remain within a tolerance zone around the final value ($\pm 10\%, \pm 5\%, \pm 1\%$, etc.)

- FV: **final value**; a fixed output value obtained for t $\rightarrow \infty$

- M: **maximum overshoot**; expressed as a percentage of the final value.

For example, in the case of a first-order system represented by the transfer function $H(s) = G/(1+sT)$, the parameters are:

- $FV = G$

- $t_R = 2.2\ T$

- $t_S = 2.2$ T (for $\pm 10\%$ FV) or $t_S = 3\ T$ (for $\pm 5\%$ FV)

- $M = 0$

The output reaches 63% of the final value for $t = T$.

2.5   Frequency response

The frequency response of a dynamic system is studied and characterized for periodic inputs of variable frequency. Figure 3 shows some typical frequency response curves for a stable system (only the gain curve is shown).
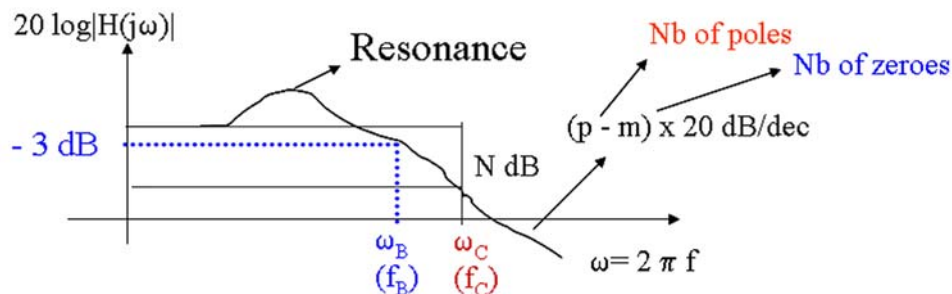

Fig. 3: Frequency response of a dynamic system (Bode plot)

The characteristic parameters of the frequency response are

- f_B: **bandwidth**; the frequency from which the zero-frequency (steady state) gain $G(0)$ is attenuated by more than 3 dB, i.e., for $\omega_B = 2\pi f_B$, $G(\omega_B) = G(0) - 3$ dB or $G(\omega_B) = 0.707 \cdot G(0)$

- f_C: **cut-off frequency**; the frequency from which the attenuation is more than N dB; i.e., for $\omega_C = 2\pi f_C$, $G(\omega_C) = G(0) - N$ dB

- Q: **resonance factor**; the ratio between the gain corresponding to the maximum of the frequency response curve and the value $G(0)$.

The asymptotic slope of the gain frequency response of a system beyond the cut-off frequency is $(p - m) \times 20$ dB/dec, where p is the number of poles and m is the number of zeros of the system.

It is important to recall that the parameters of the time and frequency responses are linked. For example, for a first-order system, the relationship between the rise time and the bandwidth is

$$f_B \cong 0.35/t_R \,. \tag{15}$$

2.6 Systems with time delay

If there is a period of time during which a state does not react to one input, the system is defined as a system with time delay. In the dynamic equation, the input $u(t)$ is replaced by $u(t - \tau)$ to take into account the fact that the input acts with a time delay of τ.

In the case of a transfer function model, the transfer function $K(s)$ of the system with time delay is the transfer function $H(s)$ of the system without delay multiplied by the transfer function of the time delay which is $e^{-s\tau}$:

$$K(s) = H(s)\, e^{-s\tau} \,. \tag{16}$$

From Eq. (16), we can deduce that there is no change of gain but that there is an addition of a phase proportional to the frequency and to the delay.

3 Closed-loop systems

3.1 State feedback (multi-input multi-output system)

In a control system, if the input is predetermined and will not change regardless of the outcome of the control, it is said to be an open-loop control system. To stabilize or to modify the dynamics of the system, it is necessary to base the input of the system on the value of the system state $X(t)$ and of the new reference input $W(t)$. As shown, the state and the input completely determine the behaviour of the system [Eqs. (1) and (2)]. Therefore a good control signal is determined by an equation of the form:

$$U(t) = H\big(X(t),\, W(t),\, t\big). \tag{17}$$

This relationship is called a control law. The best control law and its implementation are determined by the optimal control theory.

In the case of linear time-invariant systems, the control law depends linearly on $X(t)$ and $W(t)$ and is of the form:

$$U(t) = W(t) + K \cdot X(t). \tag{18}$$

where K is a constant matrix called a feedback gain matrix.

Figure 4 summarizes the effect of introducing a linear feedback. The new dynamic matrix is thus $A_k = A + B \cdot K$. The correct choice of the matrix K improves the stability and the dynamics of the system.

The controllability of the system allows the arbitrary placing of the poles in a closed-loop. Once again, the saturations, mechanical or electrical constraints, etc. of the system should not be neglected. Note that the state feedback does not change the zeros of the system. The state feedback is a generic tool stabilizing and modifying the dynamics of a multi-input multi-output (MIMO) system. It takes care of the regulation of the system but not of the tracking of references.

State feedback is much used for power converter control; for example, to stabilize and to improve the dynamics of an un-damped filter [4].
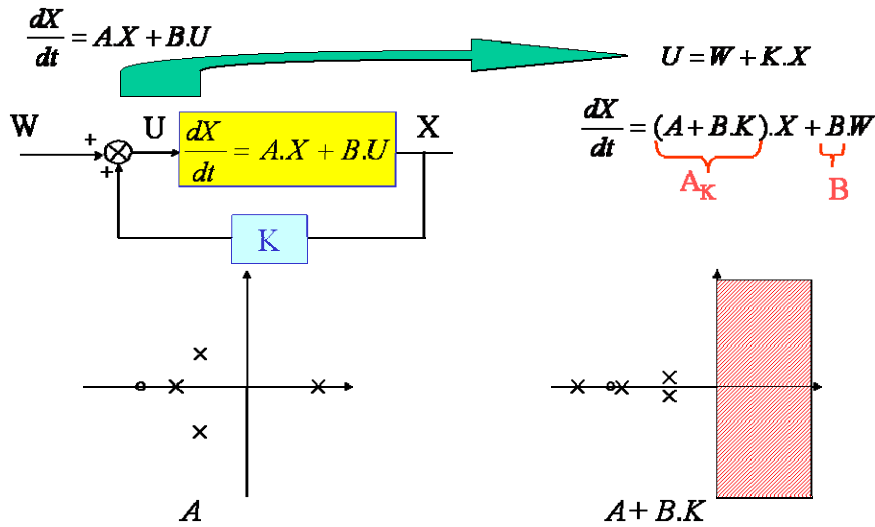
Fig. 4: State feedback stability

To track the references and to reject perturbations or disturbances, the control is a function of the difference between the references and the measured values of the controlled variables. Figure 5 shows the case of a mono-input mono-output system.
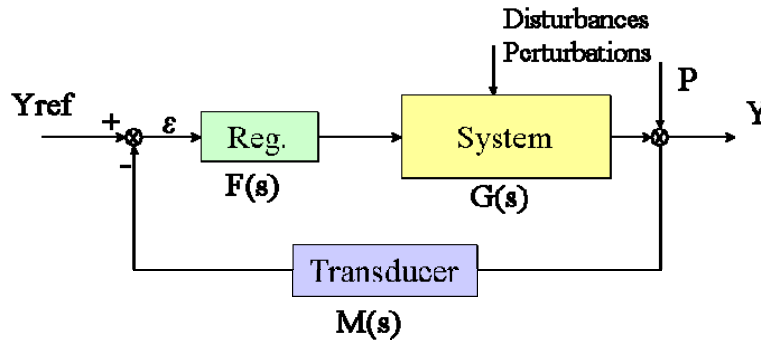

Fig. 5: Closed-loop system

If the transfer function of the system is $G(s)$, the open-loop function of the system with the controller and the transducer is $H(s) = F(s) \cdot G(s) \cdot M(s)$. The closed-loop transfer function is

$$H_{\mathrm{CL}}(s) = \frac{F(s) \cdot G(s)}{\left[1 + F(s) \cdot G(s) \cdot M(s)\right]}.$$

(19)

To obtain a zero steady-state error in closed-loop when the reference is constant, the open loop transfer function $H(s)$ must contain the internal model of the reference, which is the transfer function that generates $Y_{\mathrm{ref}}(t)$ from the Dirac impulse $\delta(t)$; e.g., step $= (1/s^2) \cdot \delta(t)$, ramp $= (1/s) \cdot \delta(t)$, sine wave $= \left[w_0/(p^2 + w_0^2) \right] \cdot \delta(t)$.

Thus when the reference is constant, the open-loop transfer function must contain an integrator. For a ramp reference, $H(s)$ must contain a double integrator in order to obtain a zero steady-state error during the ramp (no lagging error).

Figure 6 summarizes the various usual margins characterizing the stability and the dynamics of a system. The figure shows the Nyquist locus; typical values are given for the different margins.
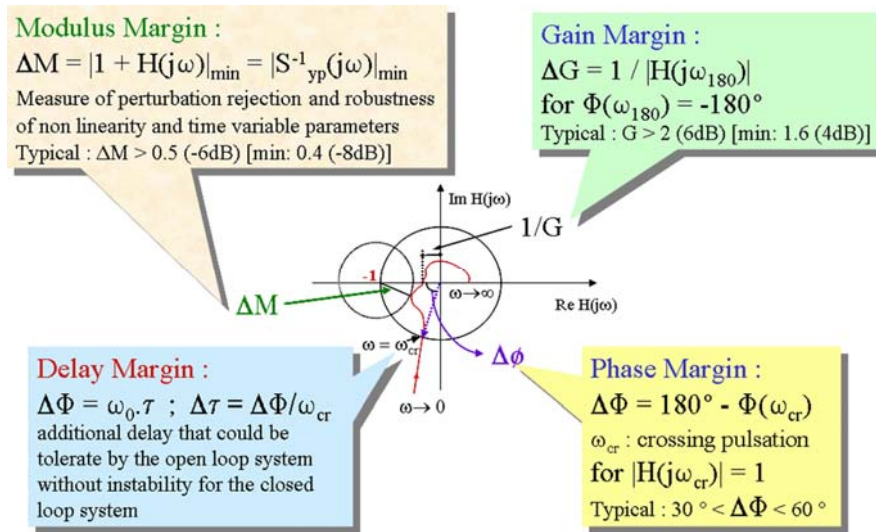

Modulus Margin :
$\Delta M = |1 + H(j\omega)|_{min} = |S^{-1}_{yp}(j\omega)|_{min}$
Measure of perturbation rejection and robustness of non linearity and time variable parameters
Typical : $\Delta M > 0.5$ (-6dB) [min: 0.4 (-8dB)]

Gain Margin :
$\Delta G = 1 / |H(j\omega_{180})|$
for $\Phi(\omega_{180}) = -180°$
Typical : $G > 2$ (6dB) [min: 1.6 (4dB)]

Delay Margin :
$\Delta\Phi = \omega_0.\tau$; $\Delta\tau = \Delta\Phi/\omega_{cr}$
additional delay that could be tolerate by the open loop system without instability for the closed loop system

Phase Margin :
$\Delta\Phi = 180° - \Phi(\omega_{cr})$
ω_{cr} : crossing pulsation
for $|H(j\omega_{cr})| = 1$
Typical : $30° < \Delta\Phi < 60°$

Fig. 6: Closed-loop system stability: different margins

Note that the modulus margin is a very useful tool for the stability but also for the perturbation rejection. The modulus margin ΔM defines the maximum value of the perturbation-output sensitivity function (see Section 3.3). More generally, a good modulus margin guarantees good values for gain and phase margins. The converse is not true.

For example, a modulus margin $\Delta M > 0.5$ implies a gain margin $\Delta G > 2$ and a phase margin $\Delta\Phi > 30°$.

Furthermore, the modulus margin defines the robustness of non-linearity and time-variable characteristics, especially in the case when these characteristics are unknown but belong to an angular sector $[a, b]$ ($b > a > 0$) (Figs. 7 and 8).
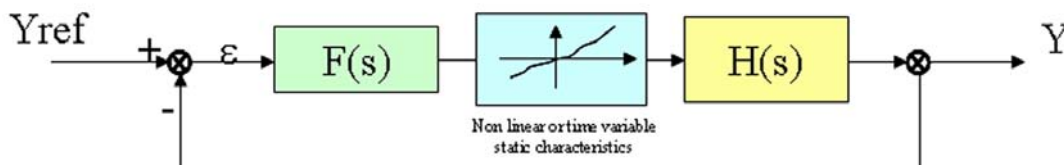

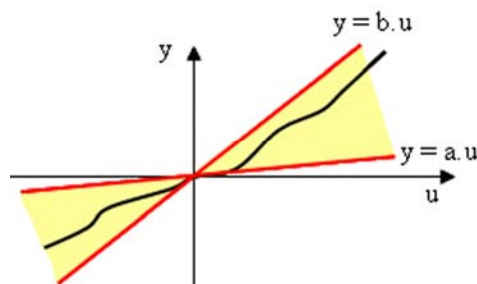**Fig. 7:** Closed-loop system with non-linear or time-variable characteristics

Fig. 8: Non-linear or time-variable characteristics

In this case, the closed-loop system is stable if the Nyquist plot leaves on the left, for ω increasing, the 'critical' circle centred on the real axis and passing through the points $(-1/b, 0)$ and $(-1/a, 0)$ without crossing the circle (Fig. 9).

For a given modulus margin ΔM, the system will tolerate non-linear or time-variable characteristics, or both, if these characteristics are located inside the sector limited by a minimum linear gain $1/(1 + \Delta M)$ and a maximum linear gain $1/(1 - \Delta M)$.
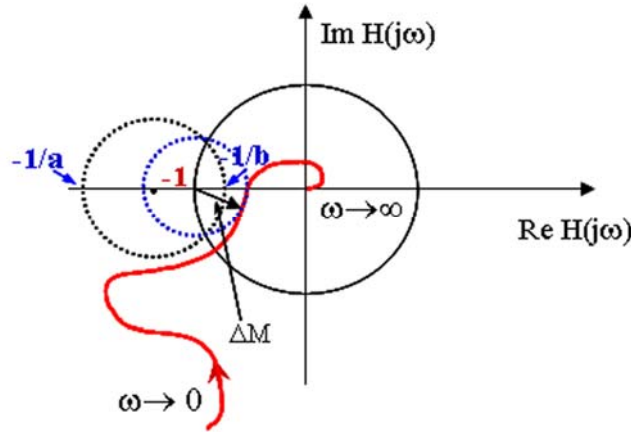
Fig. 9: Circle stability condition

3.2 Perturbation rejection

An important function is the perturbation-output sensitivity function:

$$S_{yp}(s) = \frac{Y(s)}{P(s)} = \frac{1}{\left[1 + F(s) \cdot G(s) \cdot M(s)\right]} . \tag{20}$$

To get a perfect rejection of the perturbation in steady state, $S_{yp}(0)$ must be equal to zero. Therefore, the controller must contain the classes of the perturbations. Furthermore, it is important not to have an amplification of the perturbation in a band of frequencies. The $S_{yp}(s)$ modulus should be limited to a given value G:

$$\forall \omega \in [0, \infty[, \ |S_{yp}(\omega)| < G . \tag{21}$$

A typical value for G is 2. If the energy of the perturbation is concentrated in a given frequency band, the $|S_{yp}(\omega)|$ should be limited in this band.

3.3 Choice of the desired performance

In order to design and tune a controller for a system, the first step is to know the dynamic model of the plant to be controlled, i.e., to have a control model. Two types of models can be chosen:

- non-parametric models: e.g., frequency response, step response, etc.

- parametric models: e.g., state equation, differential equation, transfer function.

A 'knowledge' type model based on the laws of physics is available, or the elaboration of an identification process is necessary [2]. In the domain of power converters, the state-space average models and equivalent average circuit models are described in Ref. [5].

Then specifications of the desired closed control loop performance should be defined for both regulation and tracking performance, i.e., the rise-time and maximum overshoot, or the bandwidth and resonance.

The choice of the desired performance, in terms of the response time (bandwidth), is linked to the dynamics of the open-loop system and to the power availability of the power converter during the transient. The acceleration of the natural response requires control peaks that are greater than the steady-state values.

The robustness of the closed-loop system is linked to the ratio f_B^{CL}/f_B^{OL}. Too high a ratio leads to a lack of robustness of the control loop; a good knowledge of the process model (high frequency identification) is needed or an adaptive control has to be used.

Taking the example of a power converter having an output voltage U and feeding a magnet, the ratio between the closed-loop dynamics and the open-loop dynamics (equal to the ratio between the closed-loop bandwidth and the open-loop bandwidth f_B^{CL}/f_B^{OL}) is directly linked to the ratio U_{max}/U_{stat}, where U_{max} is the maximum output voltage of the power converter and U_{stat} is the maximum steady-state voltage ($U_{stat} = R \cdot I_{max}$).

The example of the LHC arc orbit corrector circuit illustrates the statement.

The magnet is a superconducting magnet with an inductance of 7 H. The resistance of the cable is 30 mΩ. Thus, the time constant T of the circuit is:

$$T = L/R = 300 \text{ s, that is to say an open-loop bandwidth } f_B^{OL} \cong 0.5 \text{ mHz.}$$

The maximum current in the circuit is 60 A and the power converter designed to feed these circuit is a switch-mode power converter with a maximum output voltage of ±8 V.

The maximum steady-state voltage U_{stat} is

$$U_{stat} = R \cdot I = 1.8 \text{ V .}$$

Thus the maximum large signal bandwidth which should be achieved is

$$U_{max}/U_{stat} = 8/1.8 \cong 4 \text{ .}$$

Therefore the highest closed-loop bandwidth f_B^{CL} achievable with an 8 V converter is $\cong 2$ mHz ($t_R = 175$ s and $dI/dt_{max} \cong 0.9$ A/s).

If a small signal bandwidth equal to 1 Hz is required:

$$f_B^{CL} \cong 1 \text{ } Hz \Rightarrow f_B^{CL}/f_B^{OL} \cong \frac{1}{0.5 \cdot 10^{-3}} = 2000 \text{ .}$$

At 1 Hz, and for all the working points, the maximum current amplitude is

$$\Delta I = [(U_{max} - U_{stat})/2000]/30 \text{ m}\Omega = 0.1 \text{ A} = 0.15 \text{ \% } I_{max} \text{ .}$$

For the LHC arc orbit corrector, on account of the large time constant of the circuit, a choice of 1 Hz for the closed-loop bandwidth leads to a current range of 0.15% of the maximum current. If a larger current range is necessary, the only solution is either to reduce the closed-loop bandwidth or to increase the output voltage of the converter, thus increasing the power of the converter with implications for size and cost.

4   Digital control system

Power specialists, education and experience in the domain of regulation mainly dealt with analog systems. Then, when they started to work with digital controllers, they very often tried to reproduce the analog world where they had all their references. Figure 10 summarizes this type of approach. The error between the reference and the output is digitized with an Analog−Digital converter (ADC) with a sampling period T_s. The output of the digital controller is converted into an analog signal by a Digital−Analog Converter (DAC) with the same sampling period. This analog signal is held constant until a new conversion is ready, i.e., constant between two sampling times: Zero Order Hold (ZOH). To reproduce an analog regulation (e.g., PID type) with the block created by the ADC, digital controller and DAC implies the use of a lowest sampling period. All the potentialities of the digital controller cannot be used because of the very short time available between two sampling times: the implemented algorithms are very simple.

What is the interest of investing in a digital controller to replace an operational amplifier? To paraphrase a famous advertisement, we could say: "It is not enough to put a tiger in your tank; you've got to add BRAINs".
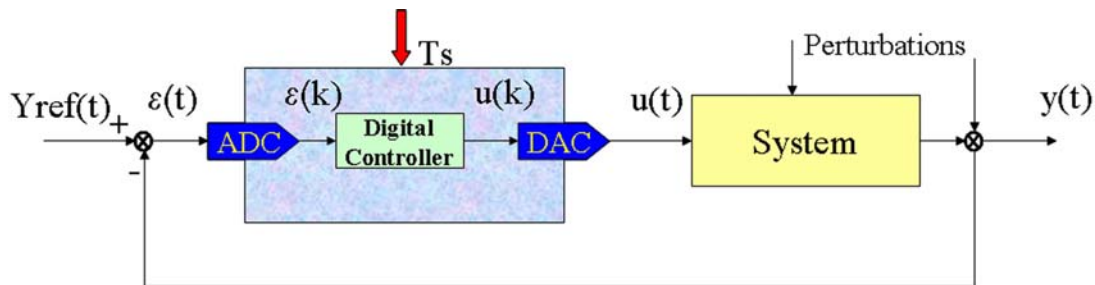

Fig. 10: Digital control of an analog-type controller

Working entirely with discrete systems is another approach. This is summarized in Figure 11. The main difference with the previous figure is that the reference is defined as a sequence of numbers: $Y_{ref}(kT_s)$ with $k \in [0,1,2,\ldots\infty[$ with the sampling period T_s. The main block now comprises the ADC, the system to be controlled, and the DAC. This block binds the sequence of numbers $Y_{ref}(kT_s)$ with the sequence of numbers $y(kT_s)$ which is the output of the AD controller.

Controller design methods are completely different. Stepping is achieved with a discrete-time model instead of with continuous-time domain. First of all, the 'discretised' system is characterized by a discrete-time model.
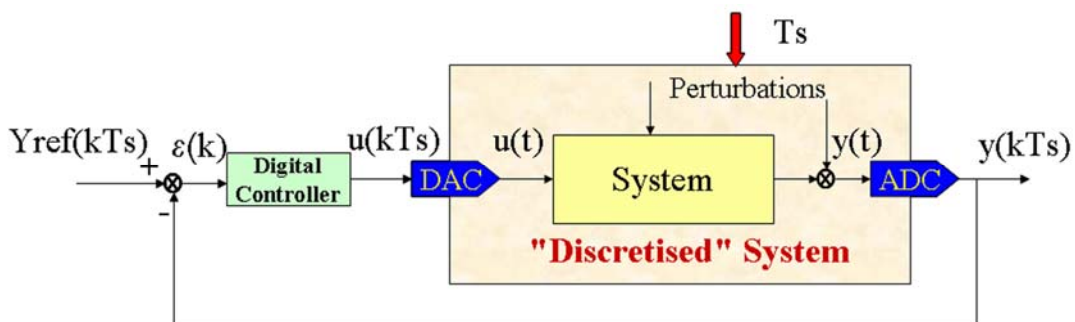

Fig. 11: Digital control system

A discrete-time model for the system is obtained from the continuous state equations (3) and (4):

$$X\left[(k+1)T_s\right] = F \cdot X(kT_s) + G \cdot U(kT_s) \tag{22}$$

$$Y(kT_s) = C \cdot X(kT_s) + D \cdot U(kT_s) \tag{23}$$

with the discrete dynamic matrices equal to:

$$F = e^{AT_s}$$
$$G = A^{-1} \cdot \left(e^{AT_s} - I \right) \cdot B . \tag{24}$$

The evolution of the state vector $X(kT_s)$ is obtained from the following equation:

$$X\left[(k_0 + n)T_s \right] = F^n \cdot X(k_0 T_s) + \sum_{j=1}^{n} F^{n-j} G \cdot U\left[(k_0 + j - 1)T_s \right] \tag{25}$$

In Eq. (25), there are two terms which correspond, respectively, to the free-state response (independent of the input vector) and to the forced-state response. The eigenvalues of the state matrix F determine the dynamics of the system.

The stability of the system can be derived from Eq. (26):

$$\lim_{n \to \infty} F^n \cdot X(k_0 T_s) = 0 . \tag{26}$$

The system is stable if the modulus of F eigenvalues is lower than 1.

Just as for the continuous domain, the three types of models can be used for the discrete model: state equations (22) and (23), algebraic equation (25) and the Z transform [6].

It is interesting to compare the step-input response of a first-order system in the continuous domain (27) and in the discrete domain (28).

$$\frac{dy}{dt}(t) = -\frac{1}{T} \cdot y(t) + \frac{G}{T} \cdot u(t) \quad \text{or} \quad H(s) = \frac{G}{1 + T_s} \tag{27}$$

$$y(kT_s) = -a_1 \cdot y\left[(k-1)T_s \right] + b_1 \cdot U\left[(k-1)T_s \right] \quad \text{or} \quad H(z) = \frac{b_1}{z + a_1} = \frac{b_1 z^{-1}}{1 + a_1 z^{-1}} . \tag{28}$$

Figure 12 shows the step response for the continuous model of a stable system ($T > 0$) and of an unstable system ($T < 0$).
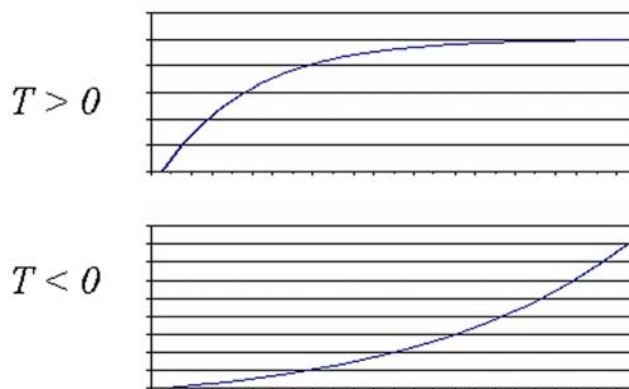

Fig. 12: Step response of continuous first-order system

Figure 13 shows the step response for the discrete model for stable and for unstable cases as well. Note that a first-order system can oscillate in the discrete domain but not in the continuous domain. A discrete first-order system can be stable while oscillating: $|a_1| < 1$ and $a_1 < 0$.
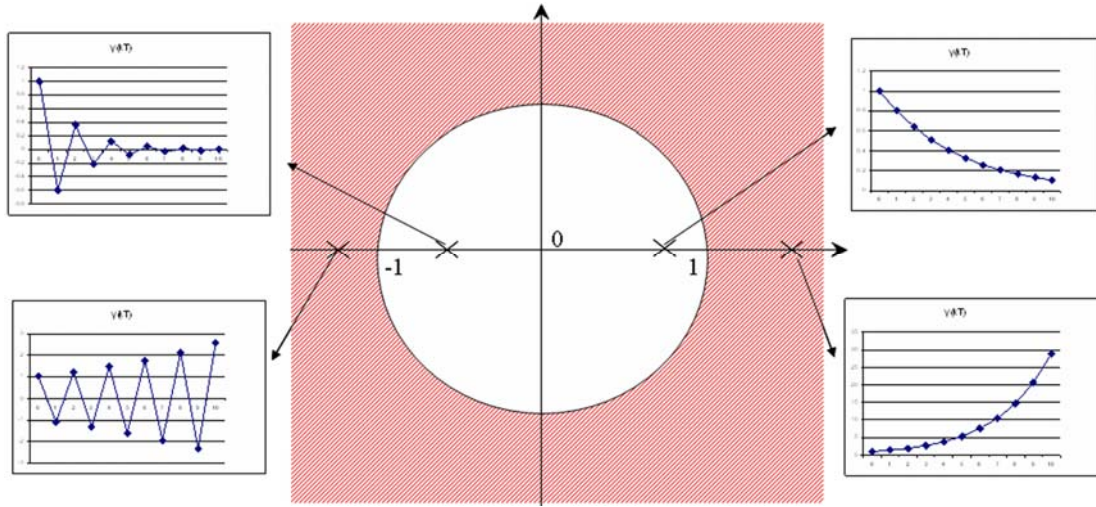

Fig. 13: Step response of discrete first-order system

4.1 Choice of sampling frequency

With the introduction of a discretised system, the constraint on the sampling frequency is relaxed. The sampling frequency is chosen in accordance with the closed-loop bandwidth.

A standard choice for the sampling frequency is between 6 to 25 times the closed-loop bandwidth [2].

$$f_s = 1/T_s \in \left[6 f_B^{CL}, \ 25 f_B^{CL} \right]. \tag{29}$$

There is no advantage to a higher sampling frequency and it could even lead to the introduction of unstable zeros [2].

The decrease of the sampling frequency takes advantage of the digital controller's power to implement more complex algorithms (than a PID), which require greater computational time, and to introduce better digital signal filtering.

4.2 RST algorithm

The general structure of a linear digital controller with time-invariant parameters can be described by the following discrete equation (a tri-branched structure known as the RST structure) (Fig. 14, Ref. [2]):

$$S\left(z^{-1}\right) \cdot u\left(kT_s\right) = T\left(z^{-1}\right) \cdot y_{\text{ref}}\left(kT_s\right) - R\left(z^{-1}\right) \cdot y\left(kT_s\right) \tag{30}$$
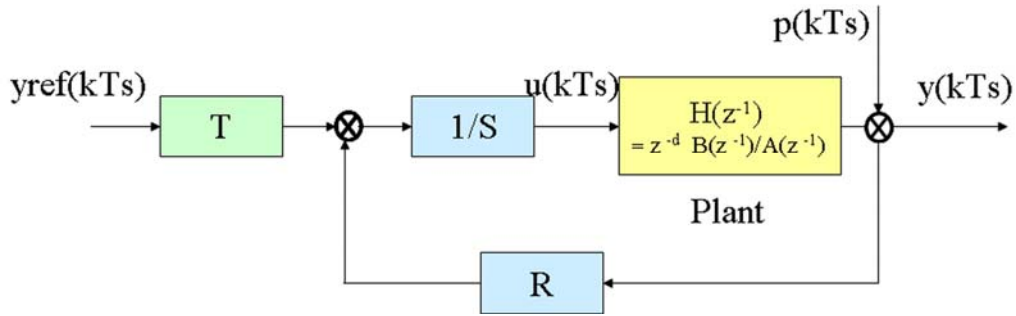
where R, S and T are z^{-1} polynomials.

Fig. 14: Generic RST control

The tracking transfer function is

$$\frac{y}{y_{ref}} = \frac{z^{-1} \cdot B \cdot T}{A \cdot S + R \cdot B \cdot z^{-1}} \tag{31}$$

and the regulation transfer function is

$$\frac{y}{p} = \frac{A \cdot S}{A \cdot S + R \cdot B \cdot z^{-1}} \quad . \tag{32}$$

Several design methods exist for the determination of the three R, S and T polynomials. The more usual methods are [2]:

– minimum variance tracking and regulation,

– tracking and regulation with weighted input (weighted control energy),

– tracking and regulation with independent objectives.

For the tracking and regulation with independent objectives method, the RST controller makes it possible to obtain the desired tracking behaviour (following the reference), independently of the desired regulation behaviour (rejection of a disturbance). This strategy can only be applied to discrete-time models with stable zeros (known as minimum-phase systems). The RST control can be evaluated by this method: R and S give the regulation behaviour, and T gives the tracking behaviour.

In this case:

$$\begin{cases} S = B \cdot H_s \\ T = A \cdot H_s + z^{-1} \cdot R \end{cases} \tag{33}$$

Then, the transfer functions become:

$$\frac{y}{y_{ref}} = z^{-1} \tag{34}$$

$$\frac{y}{p} = \frac{A \cdot H_s}{A \cdot H_s + R \cdot z^{-1}} \tag{35}$$

The regulation dynamics is defined by the R and H_s polynomials. The tracking dynamics are obtained by placing the desired transfer function between the reference and the T polynomial.
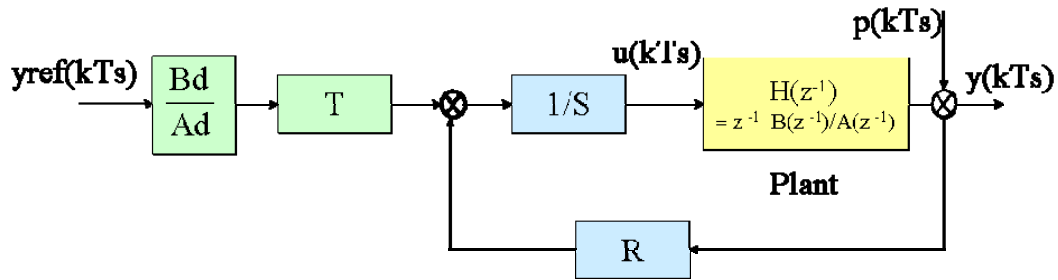
Fig. 15: Tracking and regulation with independent objectives

With some block manipulations, it can be demonstrated that the diagram of Fig. 15, is equivalent to the diagram of Fig. 16: a regulation control with a feedforward action.
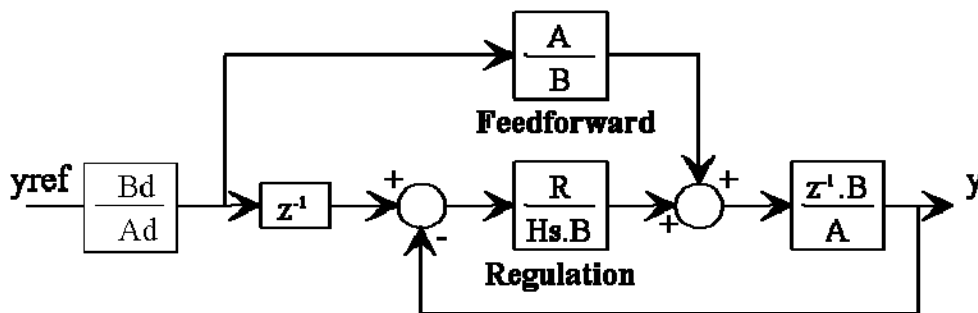

Fig. 16: Regulation control with a feedforward action.

As already said, this method can only be applied to discrete-time models with stable zeros. Unstable zeros may appear as a result of a sampling period too small for continuous-time systems with a difference in degree greater than two between the numerator and the denominator of the system transfer function [7].

4.3   Summary

The steps to design a digital controller are summarized as follows:

– Choosing the closed-loop performance [(f_B^{CL} and Q) in the frequency domain or (t_r and M) in the continuous domain)]. This choice should be based on the open-loop bandwidth frequency f_B^{OL} and on the power of the actuator. The robustness linked to the ratio f_B^{CL}/f_B^{OL}, the internal saturation and the controllability of the system should be studied.

– Choosing the sampling frequency f_s in accordance with the f_B^{CL} and respecting $f_s \in [6f_B^{CL}, 25f_B^{CL}]$.

– Computing the discrete model $H(z^{-1})$ with the chosen sampling frequency.

– Determining the parameter of the polynomials R, S and T.

– Providing anti-aliasing filters. An over-sampling frequency (multiple of the sampling period) can be used for the ADC to alleviate the analog filters. The sampled signal is passed through a digital anti-aliasing filter followed by a frequency divider to respect the defined sampling frequency (Fig. 17).
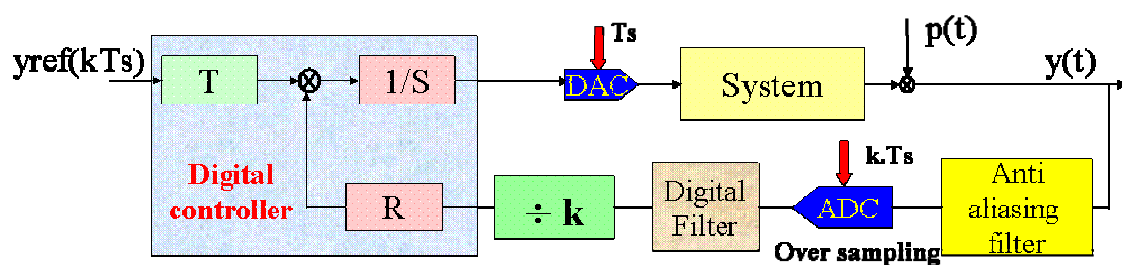
Fig. 17: Digital control system with over-sampling

5   Precision

The term 'precision' should not be used for 'accuracy'. It is only a generic term covering the following terms: accuracy, reproducibility and stability which are defined below.

Before defining these terms, it is useful to recall a few basic definitions:

a) p.p.m.: part per million = $10^{-6} \cong 2^{-20}$

b) Nominal current ($I_{nominal}$): Normal maximum value for a circuit. It is often not the maximum current of the power converter feeding the circuit. All the precision properties are defined relative to the nominal current.

c) p.p.m. of nominal: $10^{-6} \times I_{nominal}$ (A).

5.1   Accuracy

Accuracy is defined as the long-term setting or measuring uncertainty taking into consideration the full range of permissible changes of operating and environmental conditions.

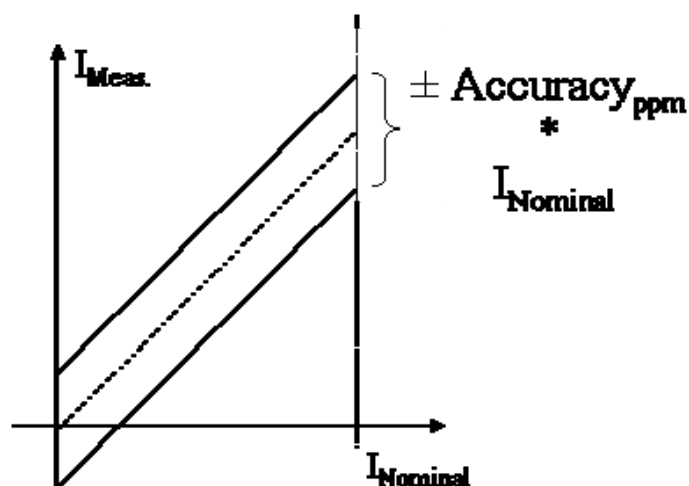Accuracy is defined by default for a given period and is expressed in p.p.m. of the nominal current (Fig. 18).

Fig. 18: Accuracy definition

5.2 Reproducibility

Reproducibility is defined as the uncertainty in returning to a set of previous working values from cycle to cycle of the machine.

Reproducibility is defined by default for a period of one day without any intervention affecting the calibrated parts (e.g. current transducer, ADCs, etc.). Reproducibility is expressed in p.p.m. of the nominal current (Fig. 19).
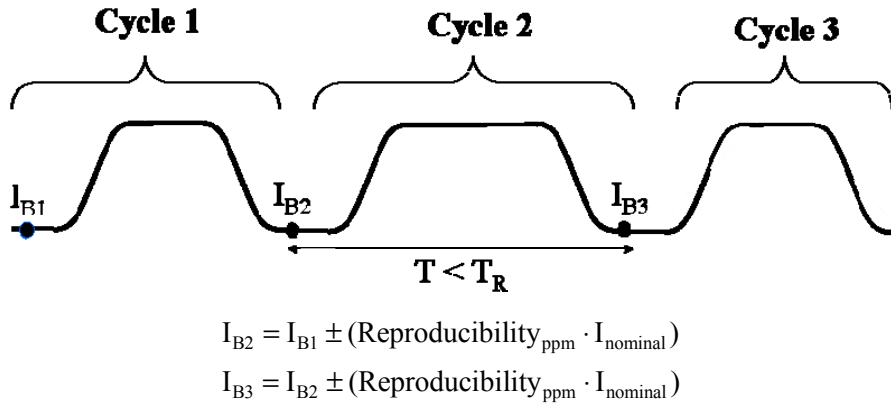

$$I_{B2} = I_{B1} \pm (\text{Reproducibility}_{ppm} \cdot I_{nominal})$$

$$I_{B3} = I_{B2} \pm (\text{Reproducibility}_{ppm} \cdot I_{nominal})$$

Fig. 19: Reproducibility definition

5.3 Stability

Stability is defined as the maximum deviation over a period with no changes in operating conditions. Stability is defined for a given period of time (e.g., half an hour). Stability is expressed in p.p.m. of the nominal current (Fig. 20).
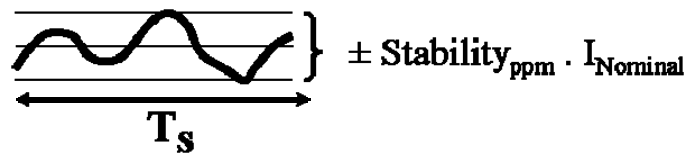

Fig. 20: Stability definition

Note: This 'stability' is a different concept than the system stability defined in Section 3.2.

5.4 Resolution

Resolution is defined as the smallest increment that can be induced or discerned.

Resolution is expressed in p.p.m. of the nominal current. The resolution is directly linked to the analog–digital conversion system.

6 LHC power converter regulation

The LHC demands an order of magnitude improvement in accuracy and reproducibility over previous accelerators [8]. The power converters must follow a very precise acceleration curve with absolutely no over or undershoot. It is therefore necessary to use a digital loop for the high-precision current loop. Furthermore, it would be difficult to realize an analog current loop with the high time constant of the magnets.

New technology was developed for the ADCs to fulfil the need for precision. The Sigma-Delta conversion principle was judged to be the most promising to meet this aim. An entirely new circuit was developed for the highest precision ADCs [9].

The digital control module receives control vectors from the central accelerator control computers and converts them to an output current reference value every millisecond. A digital regulation loop residing also in this module compares the reference value and the ADC output to calculate periodically (10–100 ms) the appropriate control value for the voltage source. This digital value is converted by a digital/analog converter (DAC) to a 0–10 V analog control signal, which is sent as a reference voltage to the voltage source, thereby closing the loop. This current control loop is designed to make the complete system behave like a 'perfect' current source (Fig. 21).
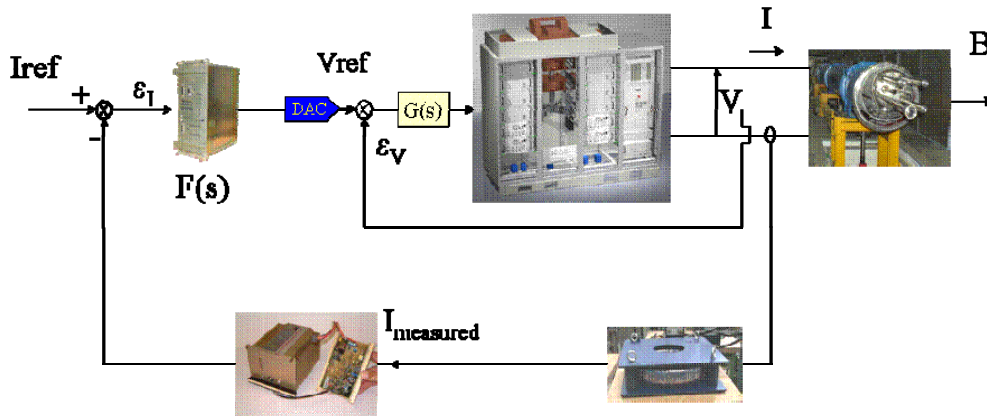

Fig. 21: LHC schematic control loops

To achieve a high rejection of mains perturbations and to operate several current sources in parallel, other control loops have been implemented at the level of the high-current power converters [10] (Fig. 22). These loops are analog regulations.

The high-precision digital current loop is a RST structure described in Section 4.2.
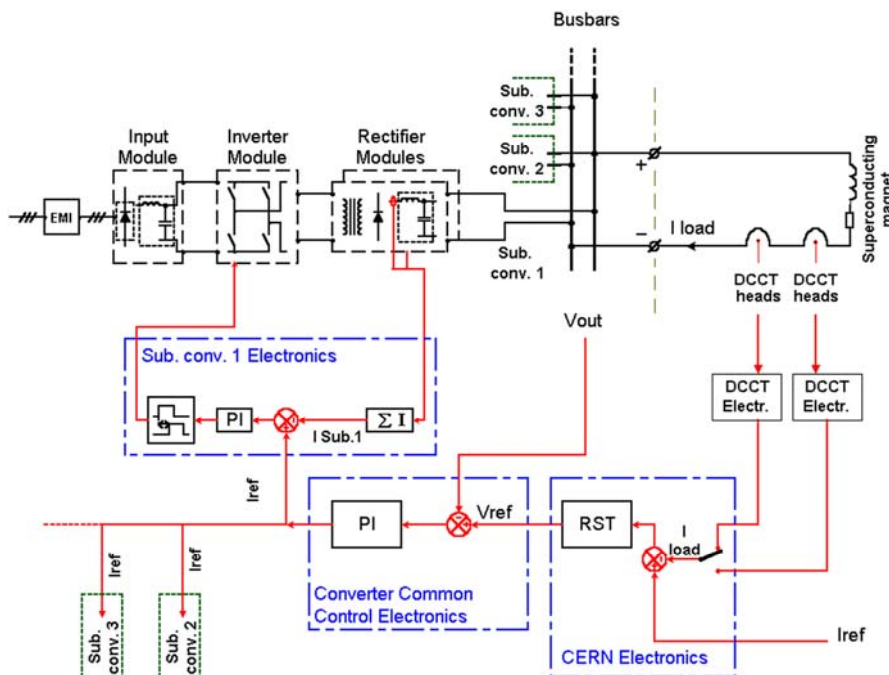

Fig. 22: Control loops of the LHC high-current power converters

With the RST controller, the desired tracking behaviour (following the reference) is obtained independently of the desired regulation behaviour (rejection of a disturbance). The RST controls are evaluated by the 'Tracking and Regulation with Independent Objectives'. This method provides a good tracking of the reference: no lagging error and no overshoot.

Figure 23 shows the first six seconds of a typical LHC ramp, illustrating the excellent resolution and accuracy of the digital control system.
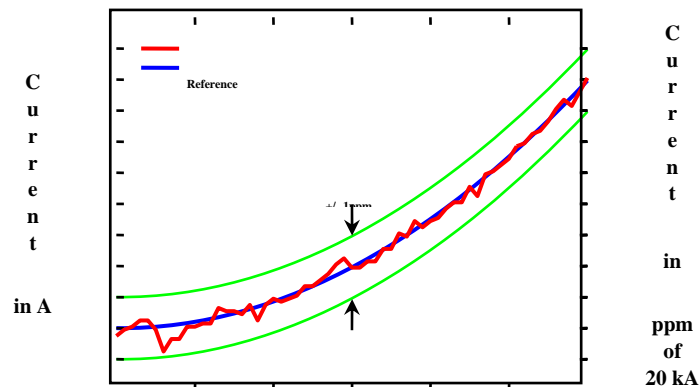

Fig. 23: The start of a short LHC ramp

Figure 24 shows the roundoff at the end of the ramp. Note that the overshoot is equal to zero.
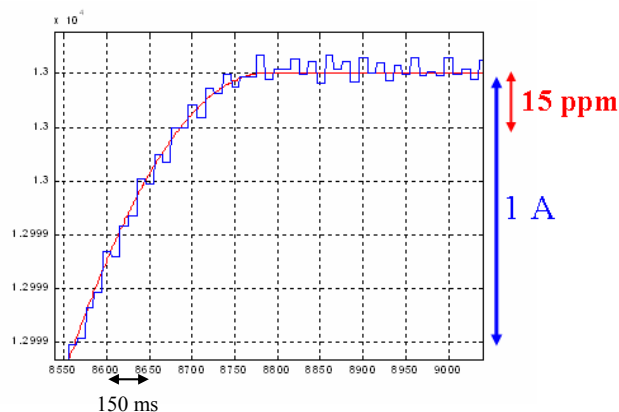

Fig. 24: End of the ramp: from 12 999 A to 13 000 A

7   Multi-input multi-output (MIMO) system to single-input single-output (SISO) system

In the domain of particle accelerators, the most general case is the feeding of one circuit by one power converter. There is one variable to regulate and one reference (generally the current).

However, on a few occasions, nested power converters are advantageous for trimming the current of different magnets. In this case, the system is a multi-input and multi-output system.

The RHIC insertion region is a good illustrative example of several layers of nested converters (Fig. 25). Shunt power converters [11] were chosen in preference to all trim magnets or individual

power supplies to reduce construction costs. The power converters in the insertion region must be tuneable and the understanding of the interaction between these power converters is critical.
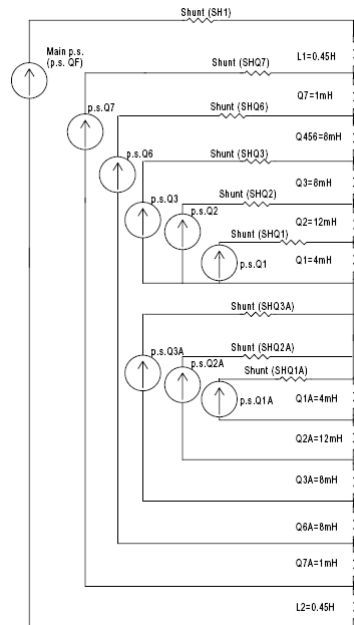

Fig. 25: RHIC sextant model

Another example is the LHC inner triplet system. It provides the final focusing of the proton beams before collision at four locations in the LHC machine. Each inner triplet consists of three quadrupole optical elements and four magnets (Q1, Q2a, Q2b, Q3) [12].

The KEK laboratory (Japan) was responsible for the design, manufacture, and acceptance tests of the Q1 and Q3 cold masses (MQXA magnet). Fermilab was responsible for the design, manufacture, and acceptance tests of the Q2a and Q2b cold masses (MQXB magnet). In 1999, it was decided that the inner triplet quadrupole magnets MQXA and MQXB would be 'mixed' in the four insertions. The two types of magnets have different design and parameters (Table 1). To optimize the powering of these mixed quadrupoles, it was decided to use two nested high-current power converters: [8 kA, 8 V] and [6 kA, 8 V], (Fig. 26).

Table 1: Inner triplet magnet parameters

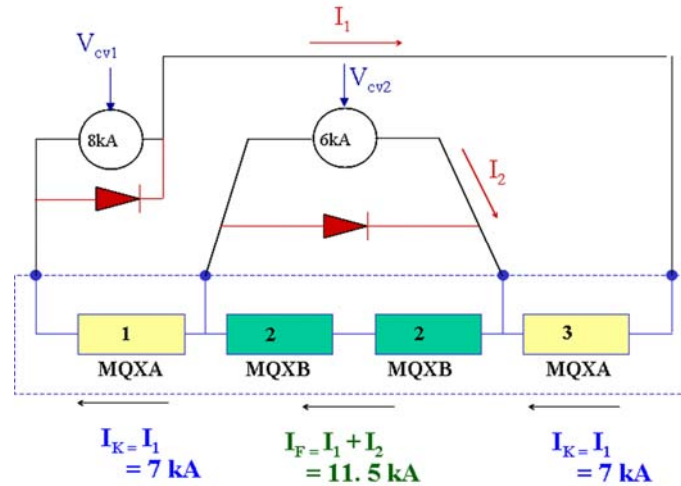|	MQXA (Q1, Q3)	MQXB (Q2a, Q2b)
Nominal gradient	205 T/m	205 T/m
Nominal current	6450 A	11 390 A
Ultimate current	6960 A	12 290 A
Inductance	90.7 mH (= L1/2)	18.5 mH (= L2/2)
Stored energy at nominal current	1890 kJ	1200 kJ

Fig. 26: LHC inner triplet powering representation

The state equations of the circuit are

$$\frac{\mathrm{d}X}{\mathrm{d}t} = A \cdot X + B \cdot U \tag{36}$$

with

$$X = \begin{bmatrix} i_1 \\ i_2 \end{bmatrix} \quad ; \quad U = \begin{bmatrix} v_1 \\ v_2 \end{bmatrix} \tag{37}$$

and

$$A = \begin{bmatrix} \dfrac{-r_1}{L1} & \dfrac{-r_2}{L2} \\ \dfrac{r_1}{L1} & -r_2 \cdot \left(\dfrac{1}{L1} + \dfrac{1}{L2} \right) \end{bmatrix}; \qquad B = \begin{bmatrix} \dfrac{1}{L1} & \dfrac{-1}{L1} \\ \dfrac{-1}{L1} & \dfrac{1}{L1} + \dfrac{1}{L2} \end{bmatrix}. \tag{38}$$

From these equations, it is clear that there is an inductive coupling between the two circuits: a variation in one voltage reference produces variations in both magnet currents. This system is a multi-input multi-output system (MIMO). This interaction leads to magnet current errors during transients. Simulations show that these errors are in the order of 10 p.p.m. at the start of the LHC ramp, which is comparable to the required reproducibility (±10 p.p.m.) for the inner triplet converters [13].

In theory, it is possible to use two independent controllers without decoupling but:

– the precision decreases with the order of the system;

– the current loops are less robust to non-linearity and to parameter changes.

To overcome these drawbacks (if possible), it is necessary to have a ratio of at least 10 between the current loop bandwidths and the frequency of the reference currents and to slow down the ramp rate or both. A better solution is to decouple the state equations.

7.1 Decoupling principle

To transform a MIMO system into two single-input single-output (SISO) systems, two matrices D and K are introduced to get a new system with diagonal state matrices:

$$\mathrm{d}X/dt = (A + B \cdot K) X + (B \cdot D) W = Ad \cdot X = Ad \cdot X + Bd \cdot W \ . \tag{39}$$

The matrices Ad and Bd are chosen as follows:

$$Ad = \begin{bmatrix} -\dfrac{r_1}{L1 + L2} & 0 \\ 0 & -\dfrac{r_2}{L2} \end{bmatrix} \dots; \quad Bd = \begin{bmatrix} \dfrac{1}{L1 + L2} & 0 \\ 0 & \dfrac{1}{L2} \end{bmatrix} \tag{40}$$

then

$$K = B^1 \cdot (Ad - A); \ D = B^1 \cdot Bd \ . \tag{41}$$

The above decoupling principle is presented for a continuous-time system; exactly the same concept can be applied to a discrete system:

$$X^* (k + 1) = F^* \cdot X^* \cdot (k) + H^* \cdot U^* \cdot (k) \tag{42}$$

with (t_s being the sampling period):

$$F* \cdot = e^{At_\mathrm{s}}; \ H* \cdot = A^{-1} \cdot \left(e^{At_\mathrm{s}} - I \right) \cdot B \ . \tag{43}$$

Fd* and Hd* are diagonal matrices:

$$X^* (k + 1) = Fd^* \cdot X^* (k) + Hd^* \cdot W^* (k) \ . \tag{44}$$

7.2 Decoupling implementation

For LHC power converters, the high-precision current loop is a digital loop implemented in a dedicated digital controller [14]. The K and D decoupling matrices can be implemented either in digital or in analog hardware (Fig. 27).
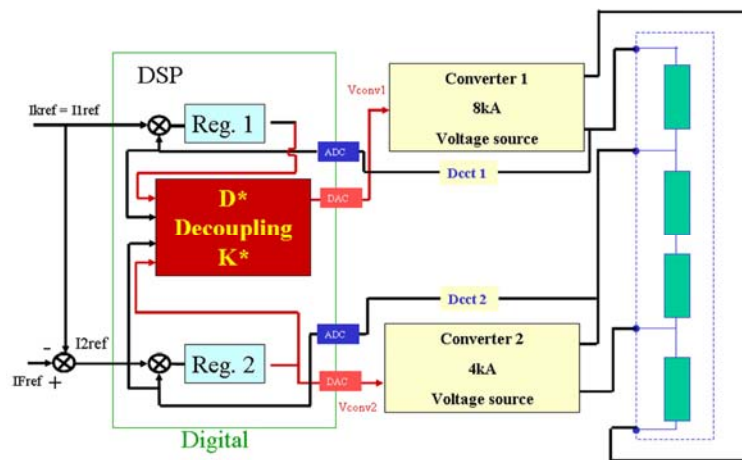

Fig. 27: Digital implementation of the decoupling matrices

To simplify and standardize the control software, it was decided to use independent, standard, LHC digital controllers for the inner triplet systems. The decoupling matrices are then implemented on an analog card located in one of the three converters (Fig. 28).
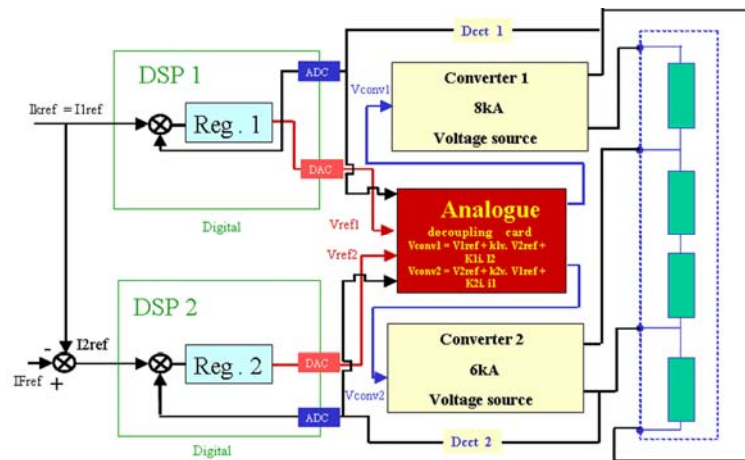

Fig. 28: Analog implementation of the decoupling matrices

The presentation of the decoupling strategy was done with a system of order two for the LHC application. For a system of order *n*, the same development could be done for the *n*-coupled circuits.

8   Conclusion

We have made a brief review of system models and closed-loop performance for continuous and discrete time domains. The important conclusion is that the design of a digital control should not be limited to the reproduction of analog loops. The best approach is to work with discrete systems exclusively and to choose the sampling frequency based on the closed-loop bandwidth. This approach was used for the design of the LHC power converters which required very high precision.

References

[1] P.M. Derusso, R.J. Roy and C.M. Close, *State Variables for Engineers* (Wiley, New York, 1965).

[2] I.D. Landau, *System Identification and Control Design* (Prentice Hall, 1990).

[3] C. Chen, *Introduction to Linear System Theory* (Holt, Rinehart and Winston, Texas, 1970).

[4] A. Beuret and F. Bordry, The control loops of the high power D.C. power converters of LEP, European Particle Accelerator Conference EPAC, Nice, France, June 1990.

[5] C. De Almeida, Methods of study of power converters for a systematic analysis, CERN Accelerator School: Power Converters for Particle Accelerators, Warrington, UK, May 2004.

[6] J.A. Cadzow and H.R. Martens, *Discrete-Time and Computer Control Systems* (Prentice Hall, 1970).

[7] F. Bordry and H. Thiesen, An RST digital algorithm for controlling the LHC magnet current, Electrical Power Technology in European Physics Research EP2, Grenoble, France, October 1998.

[8] LHC Design Report, Vol. I, CERN-2004-003 (June 2004).

[9]   J.G. Pett, A high accuracy 22-bit sigma-delta converter for digital regulation of superconducting magnet currents, 3rd Int. Conference on Advanced A/D and D/A Conversion Techniques and their Applications, Glasgow, UK, 1999, pp. 46–49.

[10] F. Bordry, G. Kniegl, V. Montabonnet, R. Pauls, H. Thiesen and B. Wolfes, Soft switching (ZVZCS) high current low-voltage modular power converter [13KA, 16V], EPE 2001, Graz, Austria, 2001.

[11] D. Bruno, G. Ganetis and R.F. Lambiase, RHIC insertion region shunt power supply simulation, Particle Accelerator Conference, New York, USA, 1999.

[12] R. Ostojic, T.M. Taylor and S. Weisz, Systems layout of the low-β insertions for the LHC experiments, Particle Accelerator Conference, Vancouver, May 1997.

[13] F. Bordry and H. Thiesen, LHC inner triplet powering strategy, Particle Accelerator Conference, Chicago, USA, 2001.

[14] I. Barnett, D. Hundzinger, Q. King and J.G. Pett, Developments in the high precision control of magnet currents for LHC, Particle Accelerator Conference, New York, USA, 1999.

Bibliography

W.A. Wolovich, *Linear Multivariable Systems* (Springer-Verlag, New York, 1974).

J. E. Gibson, *Nonlinear Automatic Control* (McGraw-Hill, 1963).

K.J. Astrom and B. Wittenmark, *Computer-Controlled Systems, Theory and Design* (Prentice Hall, 1984).

K.J. Astrom and B. Wittenmark, *Adaptive Control* (Addison-Wesley, 1989).

A. Oppenheim and R.W. Schafer, *Discrete-Time Signal Processing* (Prentice Hall, 1989).